Design and Validation of a Linear Parameter Varying Localization System *

João Barbosa[1], Carlos Cardeira[2], Paulo Oliveira[3], Pedro Batista[4] and Carlos Silvestre[5]

Abstract— This paper proposes and experimentally validates a landmark-based absolute mobile robot localization system, composed by two filters, one for attitude estimation and the other for position estimation. The estimation is carried out in the body-frame allowing for the model kinematics to be LPV (Linear Parameter Varying), thus using no approximate linearisation. The resultant estimators respect GAS (globally asymptotically stable) error dynamics, are parametrized by odometry data and corrected by landmark position and attitude measurements provided by an on-board RGB-D (red, green, blue and depth) sensor. Experiments were carried out, making use of a wheeled mobile robot and a Qualisis Motion Tracking System for ground-truth validation. Attitude and position as well as linear and angular slippages, both proven observable, are estimated, resulting in an effective real-time localization system without requiring the landmark to be always visible. Error convergence is achieved regardless of the initial estimate of both position and attitude, validating the system global stability.

I. INTRODUCTION

The problem of localization of mobile robots is one important challenge to the scientific community. The robots have to be able to use the sensors on-board, which often consist of optical encoders, mono and stereo cameras, gyroscopes, accelerometers, laser range-finders as well as others [1], in order to localize themselves in the environment, thus knowing its position in some global frame or in any local frame of interest. This localization is always needed if the robot is to autonomously plan its motions that go towards the satisfaction of a certain goal. The particular task of mobile robot is the main driver in the choice of the kind of localization needed, ranging from a topological kind of localization [2][3], often aided by a structured map or other representation of the environment, to a scenario where the robot may have to build its own map of the surroundings while simultaneously localizing itself in it, solution that is widely known as SLAM [4][5]. The latter are usually based in particle filters or extended Kalman Filters. The proposed strategy consists of a sensor-based localization system that yields the position of a certain feature or landmark in the robot frame with the use of a RGB-D (red, green, blue and depth) camera, thus allowing for an intuitive interaction of

[1]IDMEC-Instituto Superior Técnico, Universidade de Lisboa, 1049-001 Lisboa, Portugal. E-mail: joao.vitor.barbosa@ist.utl.pt

[2]IDMEC-Instituto Superior Técnico, Universidade de Lisboa,1049-001 Lisboa, Portugal. E-mail: carlos.cardeira@ist.utl.pt

[3]IDMEC and ISR-Instituto Superior Técnico, Universidade de Lisboa, 1049-001 Lisboa, Portugal. E-mail: p.oliveira@dem.ist.utl.pt

[4]ISR-Instituto Superior Técnico, Universidade de Lisboa, 1049-001 Lisboa, Portugal. E-mail: pbatista@isr.ist.utl.pt

[5]ISR-Instituto Superior Técnico, Universidade de Lisboa, 1049-001 Lisboa, Portugal and Department of Electrical and Computer Engineering, Faculty of Science and Technology, University of Macau, Macao. E-mail: cjs@isr.ist.utl.pt
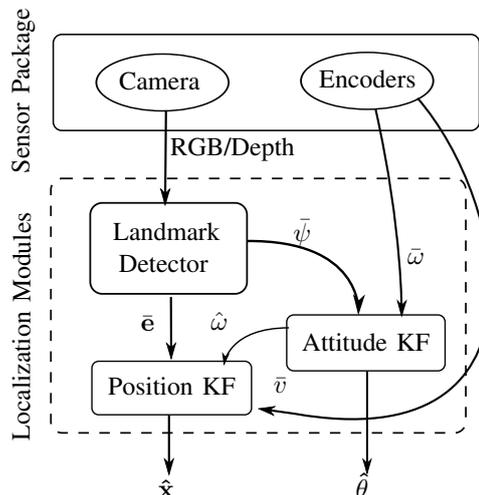
Fig. 1: Estimator Modules

the robot with its close surroundings. The purpose of this method is: i) to tackle some problems present in a number of localizers by reducing the consistency and accuracy issues caused by approximate linearisation, as is the case in any EKF based localization system, namely EKF-SLAM [6][7], and ii) to complement their functionality, allowing for a modularized approach to a specific mission. This estimator takes advantage of the independence between the attitude and position of a feature relative to the body-fixed frame, thus preventing the attitude errors from augmenting the position estimation error. The system kinematics are LPV (Linear Parameter Varying), thus allowing for GAS error dynamics in the estimators since the kinematics are not linearised for the estimation process. Angular and linear slow time varying slippages are also shown to be observable when used to augment the state, as in [8][9]. The most obvious uses for the work here described are the design of automated docking systems and possibly the application of the linear estimator apparatus to body-based SLAM algorithms, hopefully mitigating consistency issues usually present in linearised systems. This work is structured as follows: the architecture is presented in Section II, where all the modules that compose the localization system are presented, followed by the robot environment formalization in Section III. Then, both attitude and position estimator modules are presented, respectively, in Section IV and Section V. Finally the experimental results are presented and analysed in Section VI, where the ground-truth used consists of data acquired from a Qualisys™ Visual Tracking System [10].

II. ARCHITECTURE

The proposed landmark-based on-board localization system, depicted in Fig. 1, is composed of three modules: i) the landmark detector module that consists of the algorithm that

will process the RGB and depth images in order to obtain measurements of the landmark position and orientation in the robot frame; ii) a sub-optimal position estimator based on a Kalman Filter; iii) an optimal attitude estimator, also based on Kalman Filter. These modules rely, as stated before, on the sensor package composed by a RGB-D camera, that will provide the landmark detector with the images, and both optical encoders attached to the wheels that provide angular and linear velocity readings. The velocity readings are, however, not derived from the encoder readings directly, but from the commands stored in the controller. The attitude and position estimation solutions are described in Section IV and Section V, respectively.

III. MODEL DESCRIPTION

The mobile robot scenario of operation under study in this work is depicted in Fig. 2, where the frame $\{I\}$ is fixed to Earth, which is considered to be stationary for the purposes of this study, thus making it an inertial frame. Frame $\{B\}$ can be defined as being attached to the vehicle and is hence designated by body-fixed frame. Both frames $\{I\}$ and $\{B\}$ are defined, respectively, by the orthonormal basis $\{^I\mathbf{i}_I, {}^I\mathbf{j}_I\} \in \mathbb{R}^2$ and $\{^I\mathbf{i}_B, {}^I\mathbf{j}_B\} \in \mathbb{R}^2$.
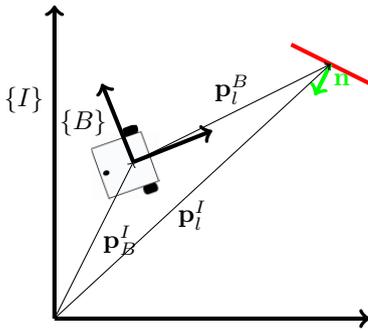
Fig. 2: Schematic of Inertial and Body-Fixed frames

In order to transform a position written in $\{B\}$ into one written in $\{I\}$, a transformation needs to be executed. The translation is defined by the body-fixed frame position in the inertial frame $\mathbf{p}_B^I$, and so the landmark position in both frames follows

$$\mathbf{p}_B^I(t) + {}^I\mathbf{p}_l^B(t) = \mathbf{p}_l^I(t), \quad (1)$$

where ${}^I\mathbf{p}_l^B(t) \in \mathbb{R}^2$ is the landmark position in $\{B\}$ expressed in $\{I\}$ and $\mathbf{p}_l^I(t)$ is the landmark position in $\{I\}$, expressed in the latter. The landmark position in the body fixed frame $\mathbf{p}_l^B(t) \in \mathbb{R}^2$ is what needs to be derived and will henceforth, for a matter of simplicity, be denoted as $\mathbf{e}(t)$.

The rotation matrix from $\{B\}$ to $\{I\}$ that simplifies (1) is denoted by ${}^I\mathbf{R}_B(t) \in SO(2)$ and respects the kinematics

$$^I\dot{\mathbf{R}}_B(t) = \mathbf{S}(\omega)\mathbf{R}(t), \quad (2)$$

where

$$\mathbf{S}(\omega) = \begin{bmatrix} 0 & -\omega \\ \omega & 0 \end{bmatrix},$$

and $\omega \in \mathbb{R}$ is the angular velocity of the body-fixed frame. The rotation ${}^I\mathbf{R}_B(t)$ will henceforth be denoted as $\mathbf{R}(t)$ for a matter of simplicity. It is straightforward to show that the inverse rotation follows a similar expression to (2) by taking

the derivative on both sides of $\mathbf{R}^T\mathbf{R} = \mathbf{I}$ and making the necessary substitutions

$$\dot{\mathbf{R}}^T(t) = -\mathbf{S}(\omega)\mathbf{R}^T(t). \quad (3)$$

IV. OPTIMAL ATTITUDE AND ANGULAR SLIPPAGE ESTIMATION

This section will focus on deriving the attitude estimator. Firstly the kinematic model will be described, giving then place for a brief observability analysis and then defining the estimator. The proposed kinematic system estimates explicitly the unavoidable angular slippage that may occur due to the lack of knowledge of the contact points with the floor as well as the lack of precision in the measurement of each wheel radius or asymmetries in mechanical construction. Here the angular slippage $s(t)$ is considered to be slow time-varying or even constant ($\dot{s} = 0$). The model that describes the attitude system is given by the kinematics and the output equations

$$\dot{\boldsymbol{\theta}}(t) = \mathbf{A}^{\boldsymbol{\theta}}\boldsymbol{\theta}(t) + \mathbf{B}^{\boldsymbol{\theta}}\omega(t) + \boldsymbol{\nu}(t), \quad (4)$$

and

$$y(t) = \mathbf{C}^{\boldsymbol{\theta}}\boldsymbol{\theta}(t) + \eta(t), \quad (5)$$

respectively, where

$$\boldsymbol{\theta}(t) = \begin{bmatrix} \psi(t) \\ s(t) \end{bmatrix},$$

$$\mathbf{A}^{\boldsymbol{\theta}} = \begin{bmatrix} 0 & -1 \\ 0 & 0 \end{bmatrix},$$

$$\mathbf{B}^{\boldsymbol{\theta}} = \begin{bmatrix} -1 \\ 0 \end{bmatrix},$$

$$\mathbf{C}^{\boldsymbol{\theta}} = \begin{bmatrix} 1 & 0 \end{bmatrix}.$$

and $\boldsymbol{\nu}(t)$ and $\eta(t)$ are the plant noise and output noise, respectively, both assumed to respect an unbounded normal distribution, i.e,

$$\boldsymbol{\nu}(t) \sim N(\mathbf{0}, \mathbf{Q}^{\boldsymbol{\theta}})$$
$$\eta(t) \sim N(\mathbf{0}, \mathbf{R}^{\boldsymbol{\theta}}).$$

This model addresses the landmark as if it is moving in the body reference system and so $\psi(t)$ represents the landmark attitude in it, which as stated before, is under the assumption that it is possible to define a unique reference system in the said landmark, and that the camera is able to detect its orientation. Assuming a constant angular velocity between two sampling instants, the state transition equation for this linear time invariant system is

$$\boldsymbol{\theta}(k+1) = \boldsymbol{\Phi}^{\boldsymbol{\theta}}(T)\boldsymbol{\theta}_k + \mathbf{G}_k^{\boldsymbol{\theta}}\omega_k + \boldsymbol{\nu}_k, \quad (6)$$

in which ω_k is the measured angular velocity obtained using the command sent to the dual-motor driver, $\boldsymbol{\Phi}^{\boldsymbol{\theta}}(T) = \exp(A^{\boldsymbol{\theta}}T_k)$, $\mathbf{G}_k^{\boldsymbol{\theta}} = \omega_k \int_0^{T_k} \boldsymbol{\Phi}^{\boldsymbol{\theta}}(T_k - \tau)\left(\mathbf{B}^{\boldsymbol{\theta}}\right)) d\tau$ and T_k is the time between samples k and $k+1$, a measured quantity, rather than a constant sampling period.

Since the continuous system is LTI, (7) is sufficient to verify the observability of the system

$$\mathcal{O}_a = \begin{bmatrix} \mathbf{C} \\ \mathbf{CA} \end{bmatrix} = \begin{bmatrix} 1 & 0 \\ 0 & -1 \end{bmatrix}. \quad (7)$$

The attitude kinematics and output system are completely defined and so it is now possible to define the dynamics of the state vector estimate, making use of the celebrated

Kalman filter,

$$\hat{\boldsymbol{\theta}}_k = \boldsymbol{\Phi}^{\boldsymbol{\theta}}(T)\hat{\boldsymbol{\theta}}_{k-1} + \mathbf{G}^{\boldsymbol{\theta}}(T)\omega_k + \mathbf{K}_k^{\boldsymbol{\theta}}\left[\bar{\psi}_k - \hat{\psi}_k\right], \quad (8)$$

where $\mathbf{K}_k^{\boldsymbol{\theta}}$ is the dynamically computed Kalman gain in time kT by using (9), (10) and (11) for each prediction or update iteration.

$$\mathbf{K}_k^{\boldsymbol{\theta}} = \mathbf{P}_k^{\boldsymbol{\theta}}\mathbf{C}^{\boldsymbol{\theta}T}\left[\mathbf{C}^{\boldsymbol{\theta}}\mathbf{P}_k^{\boldsymbol{\theta}}\mathbf{C}^{\boldsymbol{\theta}T}\right]^{-1}, \quad (9)$$

$$\mathbf{P}_{k|k-1}^{\boldsymbol{\theta}} = \boldsymbol{\Phi}_k^{\boldsymbol{\theta}}\mathbf{P}_{k-1|k-1}^{\boldsymbol{\theta}}\boldsymbol{\Phi}_k^{\boldsymbol{\theta}T} + \mathbf{Q}_k^{\boldsymbol{\theta}}, \quad (10)$$

$$\mathbf{P}_{k|k}^{\boldsymbol{\theta}} = (\mathbf{I} - \mathbf{K}_k^{\boldsymbol{\theta}}\mathbf{C}_k^{\boldsymbol{\theta}})\mathbf{P}_{k|k-1}^{\boldsymbol{\theta}}(\mathbf{I} - \mathbf{K}_k^{\boldsymbol{\theta}}\mathbf{C}_k^{\boldsymbol{\theta}T}) + \mathbf{K}_k^{\boldsymbol{\theta}}\mathbf{R}_k^{\boldsymbol{\theta}}\mathbf{K}_k^{\boldsymbol{\theta}T}. \quad (11)$$

V. SUB-OPTIMAL POSITION AND LINEAR SLIPPAGE ESTIMATION

In order to have a localization system working in $\{B\}$, as stated above, we need to be able to express $\dot{\mathbf{e}}(t)$ for the position of the landmark kinematic derivation. After having completely defined the model of the robot environment in Section III, we start by expressing the robot's position in $\{I\}$ kinematics in (12)

$$\dot{\mathbf{p}}(t) = {}^I\mathbf{R}_B(t)\mathbf{u}(t), \quad (12)$$

where $\mathbf{u}(t) = [v(t)\ 0]$ and $v(t) \in \mathbb{R}$ is the robot velocity in the body-fixed frame. By expressing the product of (1) by $\mathbf{R}^T$ we get the position $\mathbf{e}(t)$ expressed in order of $\mathbf{p}_l$ and $\mathbf{p}$ each corresponding to the landmark position and $\{B\}$ position in $\{I\}$ (respectively $\mathbf{p}_l^I$ and $\mathbf{p}_B^I$).

$$\mathbf{e}(t) = \mathbf{R}(t)^T(\mathbf{p}_l(t) - \mathbf{p}(t)), \quad (13)$$

which, once the time derivative is taken gives

$$\dot{\mathbf{e}} = \dot{\mathbf{R}}^T(t)(\mathbf{p_l}(t) - \mathbf{p}(t)) + \mathbf{R}^T(t)(\dot{\mathbf{p}}_l(t) - \dot{\mathbf{p}}(t)). \quad (14)$$

Considering that the landmark will be static in the inertial reference system, the term where $\dot{\mathbf{p}}_l(t)$ will be dropped, and by using (13) and (12) in (14) we get

$$\dot{\mathbf{e}} = -\mathbf{S}(\omega)\mathbf{R}^T(t)(\mathbf{p}_l(t) - \mathbf{p}(t)) - \mathbf{R}^T(t)\dot{\mathbf{p}}(t), \quad (15)$$

and if we further use the substitutions of (13) and (12) we will get the simplified equation in (16)

$$\dot{\mathbf{e}}(t) = -\mathbf{S}(\omega)\mathbf{e}(t) - \mathbf{u}(t). \quad (16)$$

It can be further assumed that the common mode velocity $v(t)$ can suffer from a biased measurement due to slippage. The velocity could then be expressed as $v(t) = \bar{v}(t) + b$ where b is the constant or slow varying bias and $\bar{v}(t)$ is the measured linear velocity, while $v(t)$ is the true linear velocity. Thus, the slippage is only considered along the longitudinal axis of the robot. An extension to consider tranversal slippage would be straightforward. If the state vector is $\mathbf{x}(t) = [\mathbf{e}^T(t)\ b(t)]^T$ then the matrix expression for the kinematics of the position will be given by (17)

$$\dot{\mathbf{x}}(t) = \mathbf{A}(\omega(t))\mathbf{x}(t) + \mathbf{B}\bar{v}(t) + \mathbf{v}(t)$$
$$= \begin{bmatrix} 0 & \omega & -1 \\ -\omega & 0 & 0 \\ 0 & 0 & 0 \end{bmatrix}\mathbf{x}(t) + \begin{bmatrix} -1 \\ 0 \\ 0 \end{bmatrix}\bar{v}(t) + \mathbf{v}(t), \quad (17)$$

where $\mathbf{v}(t) \in \mathbb{R}^3$ is the white plant noise caused by the model uncertainty and follows the following properties

$$E[\mathbf{v}(t)] = 0, \quad \forall t \in \mathbb{R} \quad (18)$$

$$E[\mathbf{v}(t)\mathbf{v}^T(\tau)] = \mathbf{Q}\delta(t - \tau). \quad (19)$$

The output equation of the system can be expressed by (20) since the camera sensor gives the landmark localization in $\{B\}$

$$\mathbf{y}(t) = \mathbf{e}(t) + \mathbf{w}(t), \quad (20)$$

where $\mathbf{w}(t)$ represents the noise generated by the camera sensor as well as the detection algorithm and has similar properties to those of the plant noise

$$E[\mathbf{w}(t)] = 0, \quad \forall t \in \mathbb{R} \quad (21)$$

$$E[\mathbf{w}(t)\mathbf{w}^T(\tau)] = \mathbf{R}\delta(t - \tau), \quad \forall t, \tau \in \mathbb{R}. \quad (22)$$

Also, both the plant and the sensor noise are uncorrelated, which can be expressed as

$$E[\mathbf{w}(\eta)\mathbf{v}(\tau)] = 0, \quad \forall \eta, \tau \in \mathbb{R}. \quad (23)$$

By taking an identical approach to the one in Section IV, the LPV discrete system is defined as

$$\mathbf{x}_k = \boldsymbol{\Phi}(\omega_k)\mathbf{x}_{k-1} + \mathbf{G}_k v_{k-1} + \mathbf{v}_k, \quad (24)$$

where the transition matrix $\boldsymbol{\Phi}_k$ is expressed by (25)

$$\boldsymbol{\Phi}_k = \exp\left(\int_0^{T_k}\mathbf{A}(\tau)d\tau\right)$$
$$= \begin{bmatrix} c(\omega_k T_k) & s(\omega_k T_k) & -\frac{s(\omega_k T_k)}{\omega_k} \\ -s(\omega_k T_k) & c(\omega_k T_k) & \frac{1-c(\omega_k T_k)}{\omega_k} \\ 0 & 0 & 1 \end{bmatrix}, \quad (25)$$

$\mathbf{v}_k$ is the discrete white noise and $\mathbf{G}_k$ is the discrete input matrix expressed in (26)

$$\mathbf{G}_k = \int_{t_{k-1}}^{t_k}\boldsymbol{\Phi}(\tau, t_{k-1})\mathbf{B}d\tau = \begin{bmatrix} -\frac{\sin\omega_{k-1}T}{\omega_{k-1}} \\ \frac{1-\cos\omega_{k-1}T}{\omega_{k-1}} \\ 0 \end{bmatrix}. \quad (26)$$

In order for the entire state vector $\mathbf{x}$ be estimated, the system needs to be observable, since the observation matrix $\mathbf{C}$ does not give information about the slippage directly. In the position model case, since the kinematics are LTV, this is assured if and only if the observability gramian $\mathbf{W_O}(t_1, t_0)$ defined by (27) is non-singular. It takes the form

$$\mathbf{W_O}(t_1, t_0) = \int_{t_0}^{t_1}\Phi^T(\tau, t_0)C^TC\Phi(\tau, t_0)d\tau$$
$$= \int_{t_0}^{t_1}\begin{bmatrix} 1 & 0 & a \\ 0 & 1 & b \\ a & b & c \end{bmatrix}d\tau, \quad (27)$$

where

$$a = -\frac{(\tau - t_0)\sin(\theta - \theta_0)}{\theta - \theta_0},$$
$$b = \frac{(\tau - t_0)(\cos(\theta - \theta_0) - 1)}{\theta - \theta_0},$$
$$c = 2\left(\frac{\tau - t_0}{\theta - \theta_0}\right)^2(1 - \cos(\theta - \theta_0)).$$

The integral does not change the matrix rank and so $rank(W_O) = 3$ which is the same as the number of states present in the state vector, thus rendering this system observable. Even if the linear movement case is considered, i.e. $\omega = 0$, it results that

$$\mathbf{W_O}(t_1, t_0)|_{\omega=0} = \begin{bmatrix} \Delta t & 0 & -\Delta t \\ 0 & \Delta t & 0 \\ -\Delta t & 0 & -\Delta t^2 \end{bmatrix}$$

and full observability is preserved.

The position estimator will perform a sub-optimal estimation since the angular velocity that parametrizes the state

transition matrix of this system is meant to take into account the angular slippage whose estimation is described in Section IV. Nevertheless, the equation that describes the estimate dynamics is similar to the one used for the attitude system estimate and is expressed by (28)

$$\hat{\mathbf{x}}_k = \mathbf{\Phi}^{\mathbf{x}}(\hat{\omega}_k, T)\hat{\mathbf{x}}_{k-1} + \mathbf{B}^{\mathbf{x}}v_k + \mathbf{K}_k^{\mathbf{x}}\left[\bar{\mathbf{e}}_k - \hat{\mathbf{e}}_k\right]. \quad (28)$$

The Kalman gain for this estimator is calculated in the exact same way as in the attitude estimator, using (9), only using the appropriate sensor noise covariance matrix $\mathbf{R}^{\mathbf{x}}$, $\mathbf{C}^{\mathbf{x}}$, $\mathbf{P}^{\mathbf{x}}$ and $\mathbf{Q}^{\mathbf{x}}$.

VI. EXPERIMENTAL RESULTS
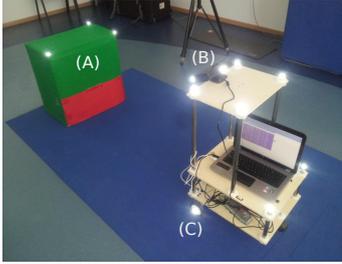
Fig. 3: Biomechanics Laboratory of Lisbon (Landmark (A), Robot prototype (B), Kinect Camera (C)).

Given the estimators proposed in this work, they must be validated with experimental results. The focus of this section is the description of the experimental setup and the analysis of the estimation errors. The ground-truth validation data acquisition system used consists of a Qualisys™ Motion Tracking [10] system that uses 14 different cameras to track the position of reflectors placed upon the mobile robot. The characteristics of the tracking system are listed in Table I.

Cameras	14 Qualisys Pro Reflex 1000
Frequency	100 Hz
Markers	19 mm diam. passive retroreflectors
Precision	<1mm after calibration

TABLE I: Qualisys Motion Tracking system characteristics.

The robot prototype and landmark setup are shown in Fig. 3. Several passive retroreflectors, which are highlighted by the camera flash, were placed on the robot and landmark to provide redundant þdata. The shown landmark serves only a purpose of validation of the theoretical localisation method. Below is a summary of the parameters and initialization of both Kalman Filters.

- Camera noise covariance: $\mathbf{R}^{\mathbf{x}} = 1 \times 10^{-2}\mathbf{I}_2$ and $\mathbf{R}^{\theta} = 1 \times 10^{-2}$
- Plant noise covariance: $\mathbf{Q}^{\mathbf{x}} = diag(4.1 \times 10^{-6}\mathbf{I}_2, 1 \times 10^{-8})$ and $\mathbf{Q}^{\theta} = diag(2 \times 10^{-5}, 1 \times 10^{-8})$
- Initial covariance matrix: $\mathbf{P}_0^{\mathbf{x}} = 1\mathbf{I}_3$ and $\mathbf{P}_0^{\theta} = 0.1\mathbf{I}_3$
- Initial conditions: $\hat{\mathbf{e}}$ and $\hat{\theta}$ were set to the real initial position, and both bias estimates $\hat{b}$ and $\hat{s}$ were set to zero.

It is also important to bear in mind the position of the camera frame $\{C\}$ relative to the body-fixed frame $\{B\}$, defined by a translation and a rotation particularized below

$$\mathbf{p}_C^B = [0.090 \quad 0.03 \quad 0.775]^T \, (m),$$

$$^B\mathbf{R}_C = \begin{bmatrix} c(\theta) & -s(\theta) & 0 \\ s(\theta) & c(\theta) & 0 \\ 0 & 0 & 1 \end{bmatrix},$$

where $\theta = 0.216 \, rad$.

A. Experimental Validation

This section comprises the localization results for two separate trajectories performed in a laboratory equipped with with a Qualisys motion tracking system. For an easier visualization, only a portion of the first trajectory tested is depicted in Fig. 4, where *Estimate* refers to a correct initialization and *Estimate 2* to a wrong one, for global stability validation. The comparison between ground truth
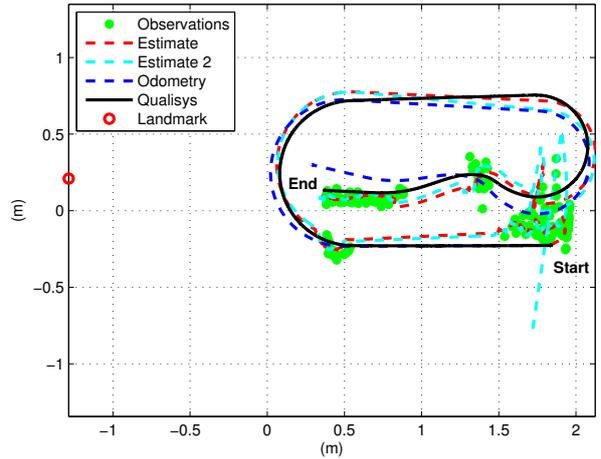
Fig. 4: Ground Truth and Estimate.

data expressed in $\{B\}$ and the estimate is depicted in Figures 5 to 7. In these results neither of the slippages were being estimated, so the open-loop is carried-out with odometry data alone. The landmark is not always visible from the robot.
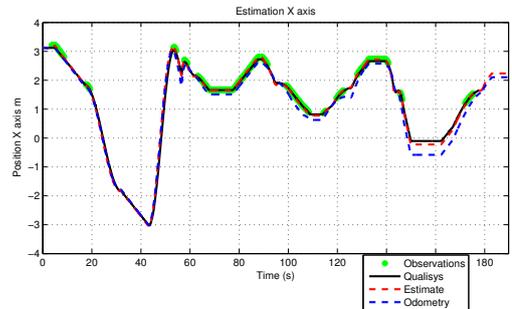
(a) Trajectory.
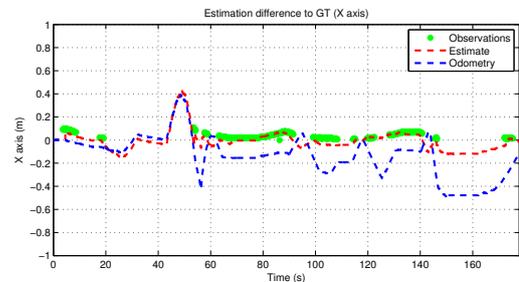
(b) Estimation error, relative to ground-truth information.

Fig. 5: Estimate and Ground Truth in X axis.

The maximum difference between the estimated trajectory
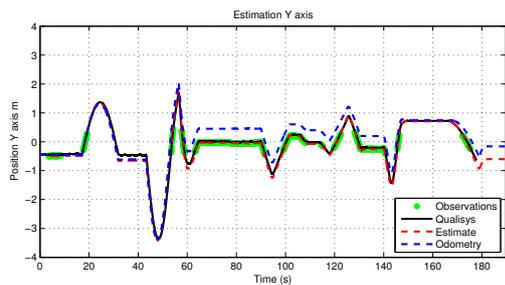
(a) Trajectory.
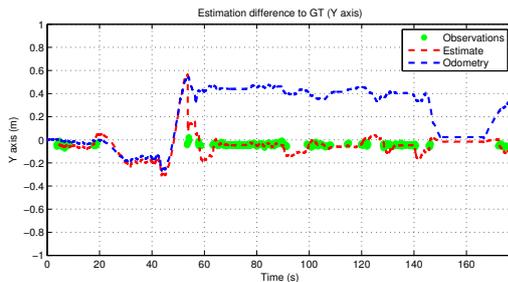
(b) Estimation error, relative to ground-truth information.

Fig. 6: Estimate and Ground Truth in Y axis.
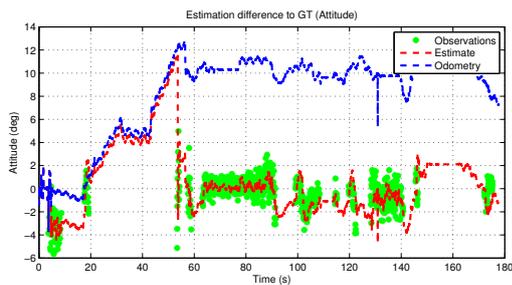
Fig. 7: Attitude estimate error, relative to ground-truth information.

occurs after an unavailability of landmarks during a period of 30 seconds and also due to sensor faulty measurements at the end of the experiment. A statistical representation of these differences can be seen in Fig. 8. When the same trajectory data is processed while also estimating the slippages, some improvement can be noticed, especially in the portion of the trajectory where both angular and linear velocities are maintained. The mentioned data set goes from 20 seconds to 50 seconds from the beginning of the experiment and the slippage estimation effect can be seen when comparing between Figures 5 to 7 with Figures 9 to 11.

Since the robot kept both velocities nearly constant, the slippage estimation that took place until the 20 second mark was suitable until the 50 second mark, allowing for a reduced open-loop estimation error. The slippage estimations are depicted in Figures 12 and 13, where the shaded areas correspond to the time periods of landmark unavailability. With the same data, a different test was conducted, this time forcing $b = -0.01\ (m/s)$. The slippage estimate behaviour is depicted in Fig. 14.

VII. CONCLUSIONS

A sensor-based positioning system based on measurements from optical encoders and from feature recognition using an RGB-D camera is proposed and experimentally validated.
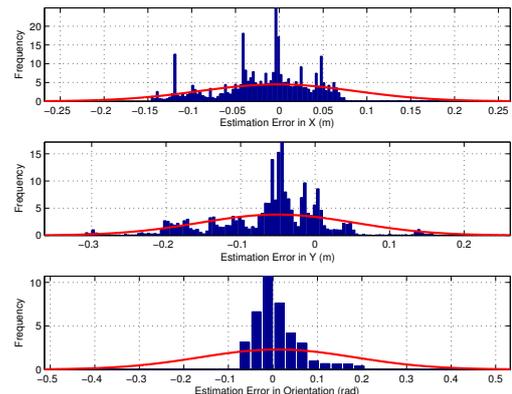
Fig. 8: Statistical study of estimation error relative to ground-truth.
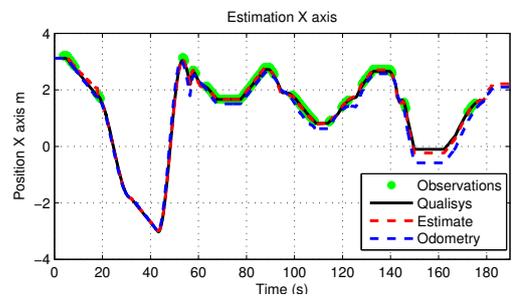
(a) Trajectory.
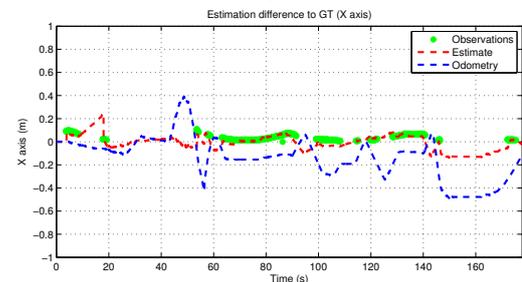
(b) Estimate error, relative to ground-truth information.

Fig. 9: Estimate and Ground Truth in X axis.

The proposed estimation system is able to localize a certain feature in the environment, tracking it even if it is not in sight, by estimating any slippage that might be occurring in the wheels for a better open-loop navigation. The Kalman filtering solution makes use of a new linear differential drive mobile robot kinematics by representing the movement of the environment in the robot frame instead of the inverse, allowing for GAS error dynamics as the system kinematics is linear, as opposed to linearised. The estimate is seen to converge rapidly once a landmark is in sight and also to be globally stable in faulty initializations or robot kidnapping scenarios. The slippage estimation contributes positively for the localization in open-loop if the robot does not change its speed too much after the slippage estimate settles. The slippage takes some time to be estimated due to the choice of values for **Q** and **R**, which were chosen so as to smooth the estimate and also avoid the slippage estimate to respond to noise or faulty measurements. This work is

(a) Trajectory.

(b) Estimate error, relative to ground-truth information.

Fig. 10: Estimate and Ground Truth in Y axis.
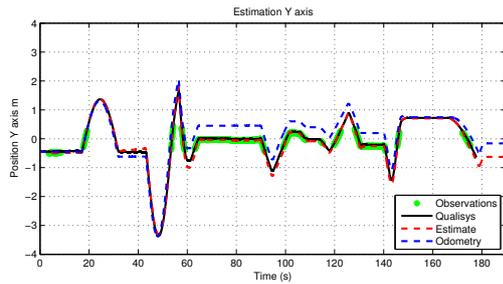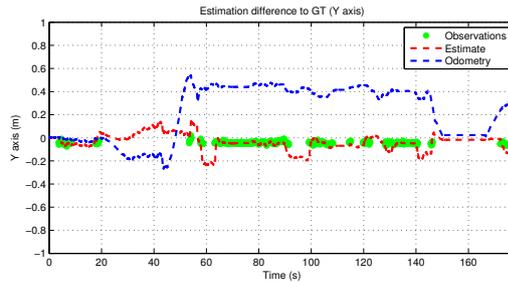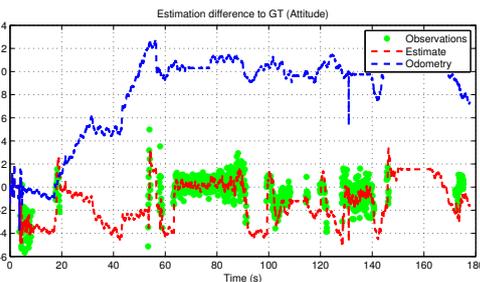
Fig. 11: Attitude Estimate error, relative to ground-truth information.

meant to be applied in a modularized approach, however a global localization can be devised by simply using several landmarks and allowing for a parallel filtering of several Kalman units, one for each landmark of interest, where a global estimator would not be able to navigate open-loop for long periods.

ACKNOWLEDGEMENTS
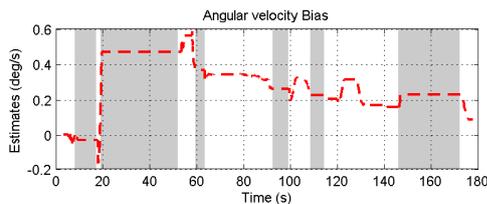
Fig. 12: Angular slippage estimation.
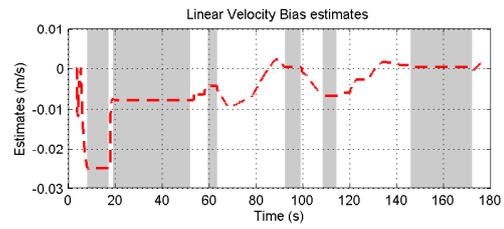
Fig. 13: Linear slippage estimation.
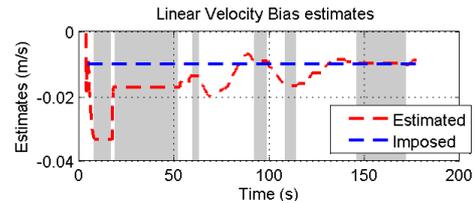
Fig. 14: Linear slippage estimation.

REFERENCES

[1] Roland Siegwart, Illah Reza Nourbakhsh, and Davide Scaramuzza. *Introduction to Autonomous Mobile Robotos*. The MIT press, 2nd edition, 2011.
[2] Paul Blaer and Peter Allen. Topological mobile robot localization using fast vision techniques. In *In Proceedings of the 2002 IEEE International Conference on Robotics and Automation*, volume 1, pages 1031–1036. IEEE, 2002.
[3] Henrik Andreasson and Tom Duckett. Topological localization for mobile robots using omni-directional vision and local features. In *Proc. IAV*. Citeseer, 2004.
[4] Tim Bailey and Hugh Durrant-Whyte. Simultaneous localization and mapping (slam): Part ii. *Robotics & Automation Magazine, IEEE*, 13(3):108–117, 2006.
[5] Hugh Durrant-Whyte and Tim Bailey. Simultaneous localization and mapping: part i. *Robotics & Automation Magazine, IEEE*, 13(2):99–110, 2006.
[6] Tim Bailey, Juan Nieto, Jose Guivant, Michael Stevens, and Eduardo Nebot. Consistency of the ekf-slam algorithm. In *2006 IEEE/RSJ International Conference on Intelligent Robots and Systems*, pages 3562–3568. IEEE, 2006.
[7] Shoudong Huang and Gamini Dissanayake. Convergence and consistency analysis for extended kalman filter based slam. *IEEE Transactions on Robotics*, 23(5):1036–1049, 2007.
[8] Pedro Batista, Carlos Silvestre, and Paulo Oliveira. Optimal position and velocity navigation filters for autonomous vehicles. *Automatica*, 46(4):767–774, 2010.
[9] Pedro Batista, Carlos Silvestre, and Paulo Oliveira. On the observability of linear motion quantities in navigation systems. *Systems & Control Letters*, 60(2):101–110, 2011.
[10] Qualisys motion capture system. http://www.qualisys.com. Accessed: 2013-07-10.
[11] José A Castellanos, José Neira, and Juan D Tardós. Limits to the consistency of ekf-based slam 1. 2004.